Scientific Research Publishing

Food and Nutrition Sciences, 2025, 16(11), 1668-1690
https://www.scirp.org/journal/fns
ISSN Online: 2157-9458
ISSN Print: 2157-944X

Natural Polyphenols from *Euterpe oleracea* Seed (açaí) Extract Prevent Brown Adipose Tissue Dysfunction and Metabolic Alterations Induced by High-Fat Diet in C57Bl/6 Mice

Dafne Lopes Beserra-Silva, Izabelle Barcellos Santos, Graziele Freitas de Bem, Beatriz Cardoso de Oliveira, Anne Caroline Alves Nogueira, Dayane Teixeira Ognibene, Cristiane Aguiar da Costa, Ângela Castro Resende*

Department of Pharmacology, Institute of Biology, Rio de Janeiro State University, Rio de Janeiro, Brazil
Email: *Angelaresende.uerj@gmail.com

How to cite this paper: Beserra-Silva, D.L., Santos, I.B., de Bem, G.F., de Oliveira, B.C., Nogueira, A.C.A., Ognibene, D.T., da Costa, C.A. and Resende, Â.C. (2025) Natural Polyphenols from Euterpe oleracea Seed (açaí) Extract Prevent Brown Adipose Tissue Dysfunction and Metabolic Alterations Induced by High-Fat Diet in C57Bl/6 Mice. *Food and Nutrition Sciences*, **16**, 1668-1690.
https://doi.org/10.4236/fns.2025.1611097

Received: September 29, 2025
Accepted: November 9, 2025
Published: November 12, 2025

Abstract

Brown adipose tissue (BAT) plays a key role in energy expenditure and is increasingly recognized as a potential target in obesity treatment. BAT dysfunction is characterized by compromised mitochondrial biogenesis and thermogenesis, as well as oxidative stress and inflammation. This study evaluated whether polyphenol-rich açaí seed extract (ASE) could prevent BAT dysfunction in C57BL/6 mice fed a high-fat (HF) diet. Male C57BL/6 mice were divided into three groups: control (10% lipid diet), HF (60% lipid diet), and HF+ASE (60% lipid diet + 300 mg/kg/day) for 12 weeks. ASE showed promising effects in preventing body mass gain, visceral adiposity, hyperglycemia, and dyslipidemia without affecting energy intake. In BAT, ASE preserved the typical multilocular morphology and prevented whitening. ASE restored the expression of thermogenic markers (UCP-1, β_3-AR) and lipolytic enzymes (ATGL, HSL, PLIN-1), as well as PPARα and mitochondrial biogenesis markers (PGC-1α, NRF1, and TFAM). Furthermore, ASE treatment reduced oxidative damage by decreasing malondialdehyde (MDA) levels and 8-isoprostane immunostaining and increased antioxidant defense through increased superoxide dismutase (SOD) activity. It also attenuated BAT inflammation by lowering MCP-1 and TNF-α expression. These results suggest that ASE mitigates obesity-induced BAT structural changes and dysfunction through its antioxidant, anti-inflammatory, and beneficial metabolic actions. These beneficial effects of ASE in BAT may represent a new target in preventing obesity.

Keywords

Euterpe, Obesity, Inflammation, Oxidative Stress, Brown Adipose Tissue

1. Introduction

The rising global prevalence of overweight and obesity constitutes a critical public health challenge closely linked to significant comorbidities. This trend is fundamentally rooted in an imbalance between energy consumption and expenditure, where sustained positive energy balance results in excessive weight gain and obesity [1]. However, effective treatments for obesity are scarce, and new therapeutic targets are needed.

Brown adipose tissue (BAT) has been widely recognized due to its unique ability to dissipate excess energy as heat, thereby contributing to metabolic balance. Evidence shows that sustained activation of BAT helps restore metabolic balance by burning excess energy as heat, making BAT a promising target for treating obesity [2]-[4].

Recent studies have explored approaches to modulate BAT and alter white fat cells by targeting key molecular markers involved in energy metabolism [5]. At the same time, obesity itself promotes the whitening of brown fat cells, causing them to lose their identity and function, which is associated with mitochondrial dysfunction and lipid accumulation in BAT [6].

A key aspect of BAT function is mitochondrial biogenesis, which involves the blend of new mitochondria from existing ones through various transcription factors and is crucial for controlling thermogenesis in BAT [7]. In obesity, mitochondrial dysfunction is characterized by reduced mitochondrial respiration and increased production of reactive oxygen species (ROS), contributing to impaired BAT activity and thermogenesis failure [8].

Additionally, obesity-related low-grade inflammation, often induced by high-fat (HF) diets, promotes BAT whitening and exacerbates oxidative stress through increased ROS production, further impairing thermogenesis [4] [9]. Considering BAT's role in energy balance, its dysfunction significantly impacts body weight regulation and represents a key target for obesity treatment.

Current pharmacological therapies often cause side effects and have limited efficacy, while natural products, such as herbal extracts, offer safer alternatives with fewer adverse effects [10] [11]. Recent evidence shows the ability of polyphenols to modulate BAT activity and thermogenesis through multiple mechanisms, mainly by increasing whole-body energy expenditure, enhancing fat oxidation, elevating non-shivering thermogenesis, and reducing body fat in humans. Beyond direct effects, polyphenols undergo metabolic transformation mediated by the gut microbiota, generating bioactive metabolites that trigger endocrine and thermogenic pathways in peripheral tissues, leading to the upregulation of key thermogenic and mitochondrial biogenesis markers [12] [13].

In this context, the plant *Euterpe oleracea* Mart. (Arecaceae), commonly known as açaí, is native to the Amazon and has attracted attention due to its high polyphenol content and antioxidant properties [14] [15]. The hydroalcoholic açaí seed extract (ASE) has been shown to contain significant levels of polyphenols, which may underlie its metabolic benefits [16]. Previous studies by our group demon-

strate that ASE can prevent body weight gain, reduce abdominal and hepatic fat, and improve hyperglycemia and dyslipidemia in HF diet-fed C57BL/6 mice [17] [18]. Studying the extract can provide valuable insights into obesity treatment and associated diseases, including natural therapies with the potential to minimize side effects, while also offering a sustainable and affordable alternative.

Therefore, this study aimed to investigate the impact of treatment with ASE on BAT remodeling, mitochondrial biogenesis markers, oxidative stress, and inflammation as possible targets for its beneficial metabolic action in a model with altered metabolism and obesity due to an HF diet (HFD).

2. Materials and Methods

2.1. Preparation of Açaí Seed Extract (ASE)

Euterpe oleracea Mart fruits were acquired from Amazon Bay (Pará State, Brazil) in the exact preserved location of Belém city. The plant was identified at the Goeldi Museum (Belém do Pará, Brazil), where a voucher specimen was deposited under the number MG 205222. The hydroalcoholic açaí seed extract (ASE) was obtained as previously described [15]. Briefly, the hydroalcoholic extract of *Euterpe oleracea* seed (ASE) was prepared by maceration using a 50:50 (v/v) ethanol-water mixture as the extraction solvent. The mixture was stored in an amber bottle at 4˚C for ten days and shaken daily at room temperature for 1 hour to enhance extraction efficiency. After the extract was filtered, it was subsequently lyophilized to obtain the dry ASE powder used in the experimental procedures. The Folin-Ciocalteu method [19] was performed to ensure that the extract contained an adequate amount of polyphenols, which was quantified as 200 mg of gallic acid equivalents (GAE) per gram of extract.

The chemical composition of the aqueous fraction residue from ASE was previously characterized by HPLC and MALDI-TOF MS [16] [20]. HPLC revealed the presence of oligomeric and polymeric proanthocyanidins (88% of total area), including catechin and epicatechin in minor amounts (see **Figure S1**) [16]. MALDI-TOF MS identified two main B-type procyanidin series: one from trimer to undecamer and another with heteropolymerization via (epi)gallocatechin units. Galloylated procyanidins were also detected, including mono-, di-, and trigalloylated trimers to pentamers (see **Figure S2**) [16]. Overall, ASE is rich in polymeric procyanidins with structural diversity, supporting its potential biological activity [16].

2.2. Animals and Diet

Animal care and experimental procedures were conducted in compliance with the Brazilian Ministry of Science, Technology, and Innovation, following the guidelines of the National Council for the Control of Animal Experimentation (CONCEA/MCTI No. 49/2021). The protocol was approved by the Animal Care and Use Committee (CEUA) of the Biology Institute at Rio de Janeiro State University (protocol number: CEUA No. 004/2021, date: 02/02/2021). All animal procedures were conducted in accordance with the NIH Guide for the Care and Use of La-

boratory Animals and the Animal Research: Reporting of *In Vivo* Experiments (ARRIVE) guidelines, version 2.0.

Four-week-old C57Bl/6 male mice were maintained in cages with three animals and controlled conditions (temperature of 21˚C ± 2˚C and a 12-hour light-dark cycle, with the light on at 6 a.m.), with free access to water and food. After an initial acclimatization period, mice were randomly assigned to either the control or high-fat diet (HFD)-induced obesity group using a computer-generated randomization list. Randomization was conducted to ensure equal group sizes and to minimize selection bias. Investigators involved in outcome assessments were blinded to group allocation where applicable. The animals (n = 36) were divided into three experimental groups (n = 12 for each group): the control group was fed a standard diet (10% fat), and HF and HF+ASE were fed a high-fat diet (60% fat). The HF + ASE group received 300 mg/kg-1d-1 of ASE by oral gavage to ensure the dose and to prevent compound oxidation, while the Control and HF groups received an equal volume of water. The sample size (n = 12 per group) was determined based on previous studies that used similar experimental designs and outcome measures in diet-induced obesity models treated with açaí extracts [21].

The diet was offered concomitantly with the treatment, and the experimental protocol lasted 12 weeks. The ASE dose and treatment duration (12 weeks) were based on previous studies from our group, which used the same HF diet model in C57BL/6 mice. These studies demonstrated metabolic alterations and significant improvements in parameters associated with metabolic syndrome following chronic administration of the extract [16]-[18]. Rhoster Indústria e Comércio Ltda (Araçoiaba da Serra, SP, Brazil) produced the diet following the standard recommendations for rodents' maintenance stated in the American Institute of Nutrition (AIN-93M). The nutritional composition of the diets used in the study is provided in **Table S1**.

This study did not include the control + ASE group because previous studies by our group with the same experimental model of obesity did not show differences in the WAT, liver, and anthropometric and biochemical parameters between the control and control + ASE groups [16].

2.3. Feed Efficiency, Food Consumption, Energy Intake, and Body Weight Measurements

The mice's food consumption was determined by their mean daily intake, which was measured by the difference between the amount of food left on the grid and the initial amount offered. Energy intake was determined from the average food intake and then multiplied by the energy content of the diets, which was 3.8 kcal/g for the control diet and 5.4 kcal/g for the HFD. To analyze the capacity to convert energy consumed from the diet into body mass, feed efficiency was considered, obtained from the relationship between total weight variation (g) and total energy ingested (kcal) [22].

Body weight was measured weekly, and the body mass gain was determined by the difference between the body mass at the end of the 12th week and the initial

body weight. As in previous studies, the sum of visceral WAT depots was determined by the Body Adiposity Index and then divided by the animal's body weight [23].

2.4. Blood Glucose Determination

The blood glucose level was measured weekly after 6 hours of fasting and evaluated using a glucometer (ACCU CHEC-Active, Model: CG, Roche) to control the development of hyperglycemia, a metabolic alteration commonly associated with obesity in this experimental model.

2.5. Euthanasia and Tissue Extraction

At the end of the treatment period, mice were anesthetized with an intraperitoneal injection of thiopental sodium (70 mg/kg). Blood was collected by cardiac puncture via a coronary artery branch into the right ventricle. Plasma was separated by centrifugation at 18,000 × g for 10 minutes at 4˚C. BAT was dissected from the interscapular region, weighed, and stored at −80˚C for the following analyses, or at Millonig formalin (10% formaldehyde, 0.14 mM sodium phosphate monobasic, 0.1 M sodium hydroxide, pH 7.2) 1:10 (w/v) for histological studies. White adipose tissue (WAT) from retroperitoneal, mesenteric, and epididymal regions was weighed to calculate the adiposity index. Retroperitoneal WAT was stored in Millonig formalin 1:10 (w/v) for histological analysis.

2.6. Biochemistry Parameters

Plasma levels of triglycerides (TG; K-117), total cholesterol (TC; K-083), and high-density lipoprotein (HDL; K-071) were determined using colorimetric kits (Bioclin, Belo Horizonte, MG, Brazil). Very low-density lipoprotein (VLDL) and low-density lipoprotein (LDL) concentrations were calculated according to previously described methods [24] [25].

2.7. Morphological Analysis in White and Brown Adipose Tissue

BAT and retroperitoneal WAT, previously fixed in Millonig Formalin, suffered proper histological processing, were sectioned at 5 μm using a rotary microtome (EasyPath, model EP-31-20091, São Paulo, SP, Brazil), and stained with hematoxylin-eosin [18]. The slides were mounted with DPX mounting medium (Sigma-Aldrich, St. Louis, MO, USA). Ten fields per slide were captured using an Olympus BX60 optical microscope (Olympus, Tokyo, Japan) equipped with an Olympus DP71 digital camera at 100× magnification using immersion oil (Type-F, Olympus, Tokyo, Japan) for BAT and 40× magnification for WAT. Image acquisition was performed using CellSens software (version 4.2, Olympus/Evident, Tokyo, Japan). The quantification was performed using the STEPanizer (Oracle Corporation, Redwood Shores, CA, USA). White adipocyte quantification was performed using the 16-point system, while brown adipocyte quantification was performed by counting the total number of nuclei within the test area.

2.8. Immunohistochemistry

BAT sections previously processed and sectioned at 5 μm were deparaffinized, rehydrated, and incubated in a humidified chamber for the procedure described previously [18]. The sections were incubated in a primary antibody (1:100 dilution in PBS) at 4˚C overnight. The signal was amplified with a biotin-streptavidin complex system Vectastain® Universal Quick Kit (PK-8800, Vector Laboratories, Burlingame, CA, USA), and the positive immunoreactions were identified after incubation with 3,3'-diaminobenzidine tetrachloride (DAB; K3466, Dako, Glostrup, Denmark). The sections were counterstained with hematoxylin and mounted with DPX mounting medium (Sigma-Aldrich, St. Louis, MO, USA). Ten non-consecutive images were captured at 100x magnification using Type-F immersion oil (Olympus, Tokyo, Japan) in an Olympus BX60 (Olympus, Tokyo, Japan) microscope equipped with a DP71 digital camera. The quantification was performed using ImageJ 1.53 (National Institutes of Health, MD, USA) with the colour deconvolution plug-in based on the H-DAB color spectrum. The primary antibodies are described in **Table S2**.

2.9. Western Blotting

BAT homogenates were used to evaluate the expression of the following biomarkers: thermogenesis (β_3-AR), lipolysis and fatty acid utilization (PPARα, PLIN-1, ATGL, and HSL), and mitochondrial biogenesis (PGC-1α and NRF1). Equal amounts of protein (30 μg) were denatured and separated by SDS-PAGE [18]. Membranes were incubated with biotinylated secondary antibodies: goat anti-mouse and goat anti-rabbit (1:5000; SouthernBiotech, Birmingham, AL, USA; Cat. No. 1021-08 and 4030-08, respectively), followed by streptavidin-HRP (1:5000; Merck Millipore, Burlington, MA, USA; Cat. No. GERPN1231). Blots were developed with an enhanced chemiluminescence kit (ECL-plus; Amersham Pharmacia Biotech, Piscataway, NJ, USA). The bands were visualized with the ChemiDoc XRS molecular imaging system (Bio-Rad, Hercules, CA, USA) and analyzed using Adobe Photoshop Elements 11, version 11.0 (Adobe Systems Incorporated). The results were expressed as arbitrary units. The primary antibodies used for Western blot analysis are presented in **Table S3**.

2.10. Determination of Oxidative Stress

Oxidative damage and antioxidant status were assessed in BAT homogenates using spectrophotometric methods. Lipid peroxidation, an indicator of oxidative damage to cell membranes, was quantified by measuring malondialdehyde (MDA) levels using a thiobarbituric acid reactive substances (TBARS) assay [26]. To evaluate the antioxidant defense system, enzymatic activities of key antioxidant enzymes were measured: superoxide dismutase (SOD) activity was determined by measuring the inhibition of adrenaline auto-oxidation [27], catalase (CAT) activity was assessed as the rate of decrease in H_2O_2 [28], and glutathione peroxidase (GPx) activity was measured by monitoring the oxidation of NADPH in the pres-

ence of H_2O_2 [29]. All measurements were performed using an Amersham Ultrospec 2100 pro spectrophotometer (GE Healthcare, Chicago, IL, USA) and normalized to the total protein content of each sample to correct for differences in protein concentration.

2.11. Statistical Analysis

Data are presented as mean ± standard error of the mean (SEM). All datasets followed a normal distribution, as verified by the Shapiro-Wilk test. Therefore, a one-way analysis of variance (ANOVA) was performed, followed by Tukey's post hoc test for multiple comparisons. All statistical analyses and graph generation were carried out using GraphPad Prism version 8.0 (GraphPad Software, San Diego, CA, USA). Statistical significance is indicated by *P* values, with $P \leq 0.05$ considered significant.

3. Results

3.1. Effects of ASE on Body Weight, Feed Efficiency, Adiposity Index, and Adipose Tissue Mass

The animals in the three experimental groups did not show statistically significant differences in body weight at the beginning of the protocol (Table 1). After 12 weeks, the ASE treatment resulted in a reduced final body weight ($p = 0.0060$), reinforcing its preventive effect on body mass gain ($p = 0.0006$) compared to the HF group.

Table 1. Effects of ASE on murinometric measurements and biochemical parameters.

	Control	HF	HF + ASE
Initial body weight (g)	21.54 ± 0.44	21.83 ± 0.34	21.24 ± 0.35
Final body weight (g)	26.25 ± 0.48	36.22 ± 0.92*	32.3 ± 1.01*&
Body Mass Gain (g)	4.71 ± 0.14	14.39 ± 0.65*	11.06 ± 0.72*&
Feed Efficiency (%)	0.53 ± 0.02	1.04 ± 0.05*	0.87 ± 0.05*&
Total Energy Intake (Kcal)	889.5 ± 15.34	1393 ± 54.76*	1272 ± 46.79*
Total Food Intake (g)	234.1 ± 4.04	257.9 ± 10.14	235.6 ± 8.67
Initial glucose (mg/dL)	156.2 ± 3.07	156.0 ± 3.73	155.6 ± 6.56
Final glucose (mg/dL)	143.3 ± 3.17	193.6 ± 6.42*	156.8 ± 3.93&
Plasma			
Total Cholesterol (mg/dL)	81.54 ± 1.77	151.6 ± 7.34*	128.2 ± 5.46*&
Triglycerides (mg/dL)	88.88 ± 1.69	95.75 ± 3.18	87.57 ± 1.79&
VLDL-C (mg/dL)	17.78 ± 0.34	19.25 ± 0.67	17.51 ± 0.36&
LDL-C (mg/dL)	3.56 ± 0.60	40.33 ± 6.91*	15.69 ± 2.18&
HDL-C (mg/dL)	60.20 ± 1.64	92.10 ± 3.45*	95.02 ± 4.5*

Values are presented as means ± SEM (n = 12 for all groups). One-way ANOVA analyses, and post-test of Tukey indicate *significantly different from the control group ($p \leq 0.05$), and &significantly different from the corresponding HF group ($p \leq 0.05$).

The ASE treatment also reduced feed efficiency ($p = 0.0090$) without changing total energy and food intake. Additionally, ASE treatment reduced the body adiposity index ($p = 0.0318$) and the visceral adipose tissue ($p = 0.0214$) and subcutaneous adipose tissue ($p = 0.0371$) weights (Table 2). However, these parameters in the HF + ASE group were still higher than those in the Control group. Thus, the BAT ($p = 0.0005$) weight was increased in the HF group, and the treatment with ASE did not change these parameters (Table 2).

Table 2. Effects of ASE on adipose tissue weight.

	Control	HF	HF + ASE
Body Adiposity Index (%)	3.58 ± 0.15	11.23 ± 0.57*	9.52 ± 0.53*&
Visceral adipose tissue weight (g)	0.64 ± 0.04	3.08 ± 0.20*	2.43 ± 0.19*&
Subcutaneous adipose tissue weight (g)	0.30 ± 0.12	1.00 ± 0.09*	0.77 ± 0.06*&
Brown adipose tissue weight (g)	0.13 ± 0.01	0.19 ± 0.01*	0.19 ± 0.01*

Values are presented as means ± SEM (n = 12 for all groups). One-way ANOVA analyses, and post-test of Tukey indicate *significantly different from the control group ($p \leq 0.05$), and &significantly different from the corresponding HF group ($p \leq 0.05$).

3.2. Effect of ASE on Blood Glucose and Plasma Lipid Profile

Initial blood glucose was similar between the groups (Table 1). However, at the end of the experimental protocol, the HF group showed an increase in final blood glucose ($p < 0.0001$), and treatment with ASE prevented this increase ($p < 0.0001$). The plasma levels of total cholesterol ($p < 0.0001$), LDL-C ($p < 0.0001$), and HDL-C ($p < 0.0001$) were higher in the HF group than in the control group. The ASE treatment decreased total cholesterol ($p = 0.0115$), triglycerides ($p = 0.0458$), VLDL-C ($p = 0.0395$), and LDL levels ($p = 0.0006$) compared to the HF group (Table 1). Additionally, it did not alter the increased levels of total cholesterol and HDL-C (Table 1).

3.3. Effects of ASE on Morphological Alterations in White and Brown Adipose Tissue

In the HF group, the average adipocyte area of WAT was increased ($p = 0.0004$) compared to the control group (Figure 1(A) and Figure 1(C)), indicating adipocyte hypertrophy in obesity. The ASE treatment prevented ($p = 0.0003$) this morphological alteration compared to the HF group (Figure 1(A) and Figure 1(C)), resembling the Control group.

The morphological analysis of BAT demonstrated that the Control group showed multilocular cells characteristic of brown adipocytes (Figure 1(B)). In contrast, the HF group presented lipid infiltration with bigger fat droplets and a significant decrease in the numerical density of nuclei per area ($p < 0.0001$) compared to the Control group (Figure 1(B) and Figure 1(D)). This alteration in the HF group exhibits a similar phenotype to that observed in WAT, indicating whitening in this group. ASE treatment prevented the increase of lipid droplets in this tissue,

presenting a multilocular structure of BAT with a significant increase in the numerical density of nuclei ($p < 0.0001$), similar to what was observed in the Control group (Figure 1(B) and Figure 1(D)).

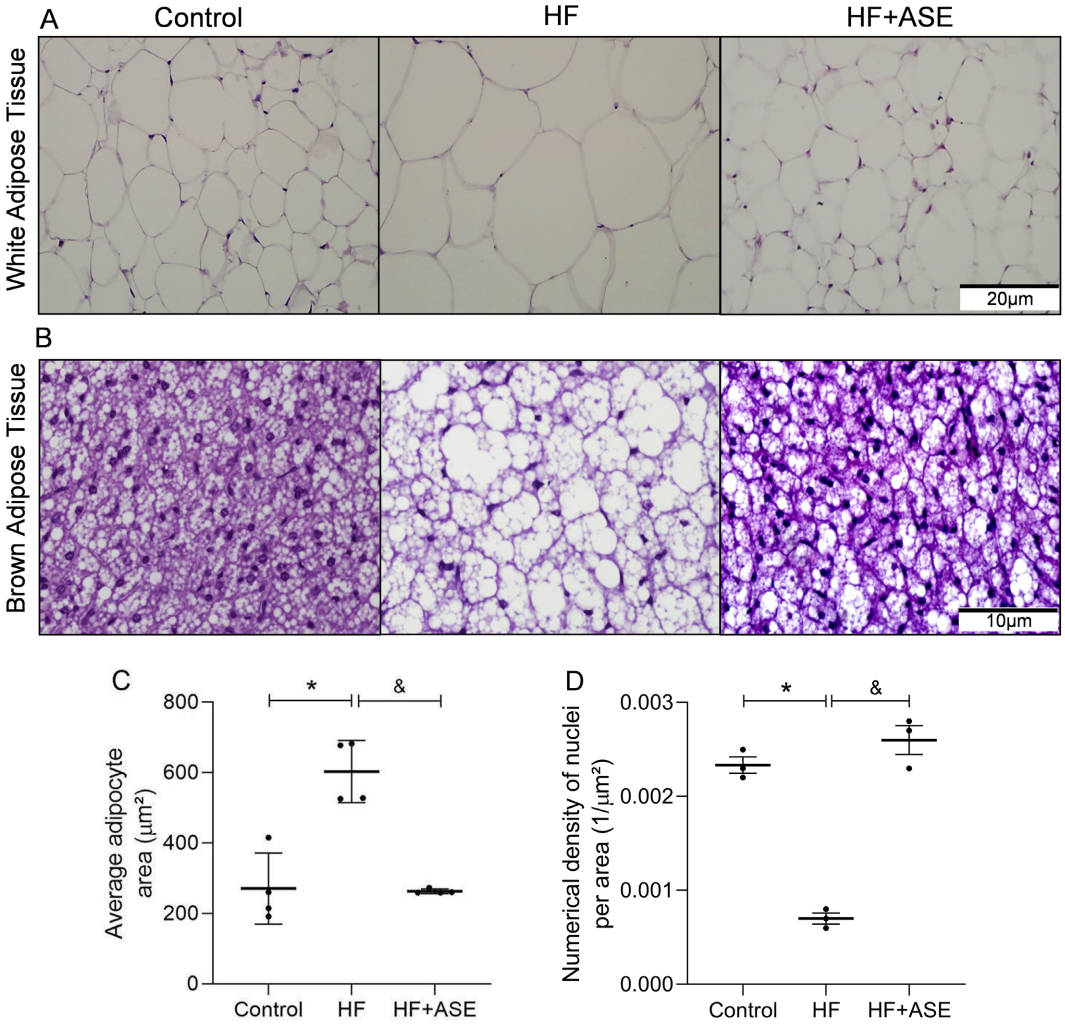

Figure 1. White and brown adipose tissue parameters and structure. Representative sections of retroperitoneal white adipose tissue (WAT) (A) and brown adipose tissue (BAT) (B), stained with hematoxylin and eosin in control, HF, and HF + ASE groups. The photomicrograph is shown at 40x with a scale bar of 20 μm in the WAT and at 100x with a scale bar of 10 μm in the BAT. Effects of ASE on the average white adipocyte area in WAT, n = 4 (C), and the numerical density of nuclei per area in BAT, n = 3 (D). Values are presented as means ± SEM. One-way ANOVA analyses, and post-test of Tukey indicate *significantly different from the control group ($p \leq 0.05$), and &significantly different from the corresponding HF group ($p \leq 0.05$).

3.4. Effect of ASE on Thermogenesis Markers

Essential proteins for thermogenesis were also evaluated. The β_3-adrenergic receptor (β_3-AR) is activated by sympathetic stimulation and inserts UCP-1 into the mitochondrial membrane. The immunostaining in BAT slides (Figure 2(A) and Figure 2(B)) showed a significant decrease in UCP-1 in the HF group compared to the Control group ($p = 0.0433$). The treatment with ASE prevented this de-

crease compared to the HF group ($p = 0.0001$) and increased this staining compared to the Control group ($p = 0.0003$). β_3-AR expression was reduced (Figure 2(C)) in the HF compared to the Control group ($p < 0.0001$), and the ASE treatment increased β_3-AR expression compared to the HF group ($p = 0.0085$) but remained minor than the control values ($p = 0.0098$).

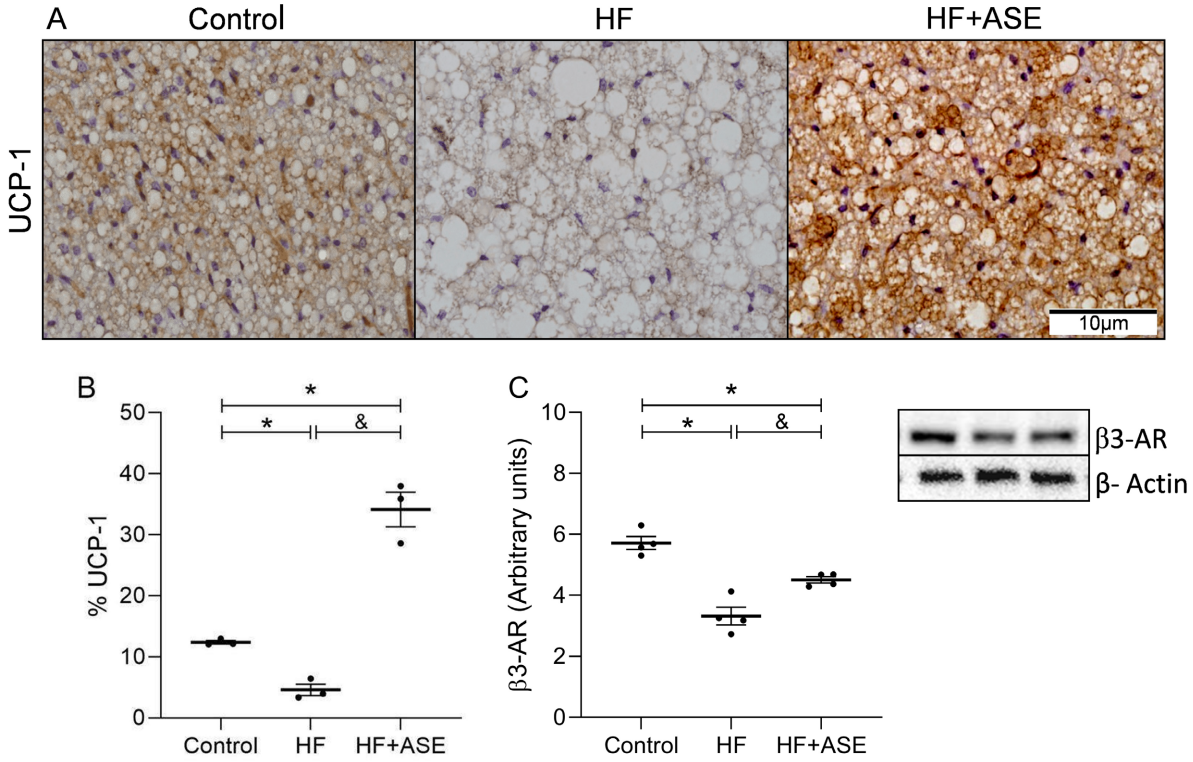

Figure 2. Thermogenesis markers. Effects of ASE on UCP-1 immunostaining (A), % of UCP-1 (B) (n = 3 for all groups), and β_3-AR expression (C) (n = 4 for all groups) in brown adipose tissue from HF-fed mice. The photomicrograph is shown at 100x, with a scale bar of 10 µm. Values are presented as means ± SEM. One-way ANOVA analyses, and post-test of Tukey indicate *significantly different from the control group ($p \leq 0.05$), and &significantly different from the corresponding HF group ($p \leq 0.05$).

3.5. Effect of ASE on Fatty Acid Utilization Markers

Free fatty acids (FFA) are required as fuel for thermogenesis. In this study, lipolytic proteins were evaluated. Western Blot analysis demonstrated a significant reduction of PPARα ($p = 0.0134$) in the HF group compared to the Control group (Figure 3(A)). There was no difference in PLIN-1 expression between the HF and Control groups (Figure 3(B)). However, compared to the HF group, ASE treatment significantly increased PPARα ($p = 0.0238$) and PLIN-1 expressions ($p = 0.0490$). The animals in the HF group showed a significant reduction in the ATGL ($p = 0.0029$) (Figure 3(C)) and HSL ($p = 0.0038$) expressions (Figure 3(D)) compared to the Control group. The treatment with ASE increased the ATGL expression compared to the Control ($p = 0.0260$) and HF ($p < 0.0001$) groups (Figure 3(C)). ASE increased HSL expression compared to the HF group ($p = 0.0339$) (Figure 3(D)).

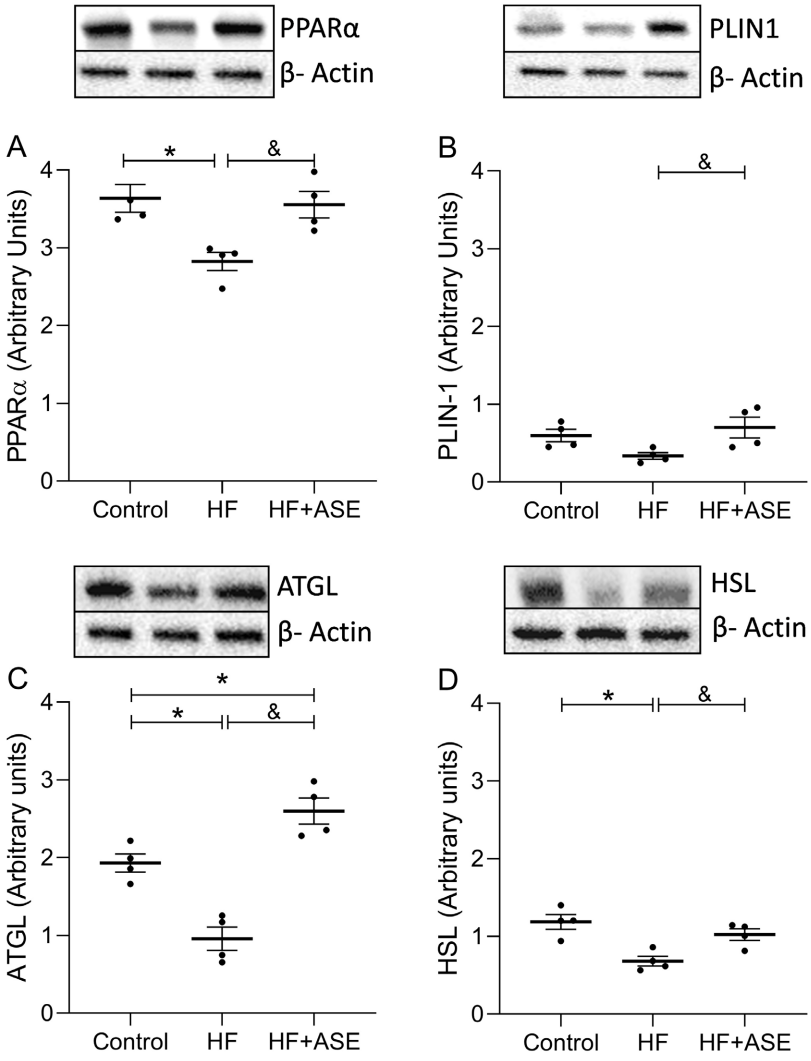

Figure 3. Fatty acid utilization markers. Effects of ASE on the expression of PPAR*α* (A), PLIN-1 (B), ATGL (C), and HSL (D) in brown adipose tissue from HF-fed mice. Values are presented as means ± SEM, n = 4 for all groups. One-way ANOVA analyses, and post-test of Tukey indicate *significantly different from the control group ($p \leq 0.05$), and &significantly different from the corresponding HF group ($p \leq 0.05$).

3.6. Effect of ASE on Mitochondrial Biogenesis Markers

In mitochondrial biogenesis, the activation of peroxisome proliferator-activated receptor-gamma coactivator (PGC-1*α*) is followed by the expression of nuclear respiratory factor 1 (NRF1), that results in the expression of mitochondrial transcription factor A (TFAM), the final effector of mitochondrial biogenesis.

Western blot analysis demonstrated a decreased expression of PGC-1*α* (p = 0.0090) and NRF1 (p = 0.0010) in the HF compared to the Control group (**Figure 4(A)** and **Figure 4(B)**), which was prevented by ASE (p = 0.0016 and p = 0.0025, respectively). In addition, the immunostaining of TFAM (**Figure 4(C)** and **Figure 4(D)**) was reduced in the HF group (p = 0.0470) compared to the Control group, and the ASE treatment prevented this reduction compared to the HF group (p = 0.0399).

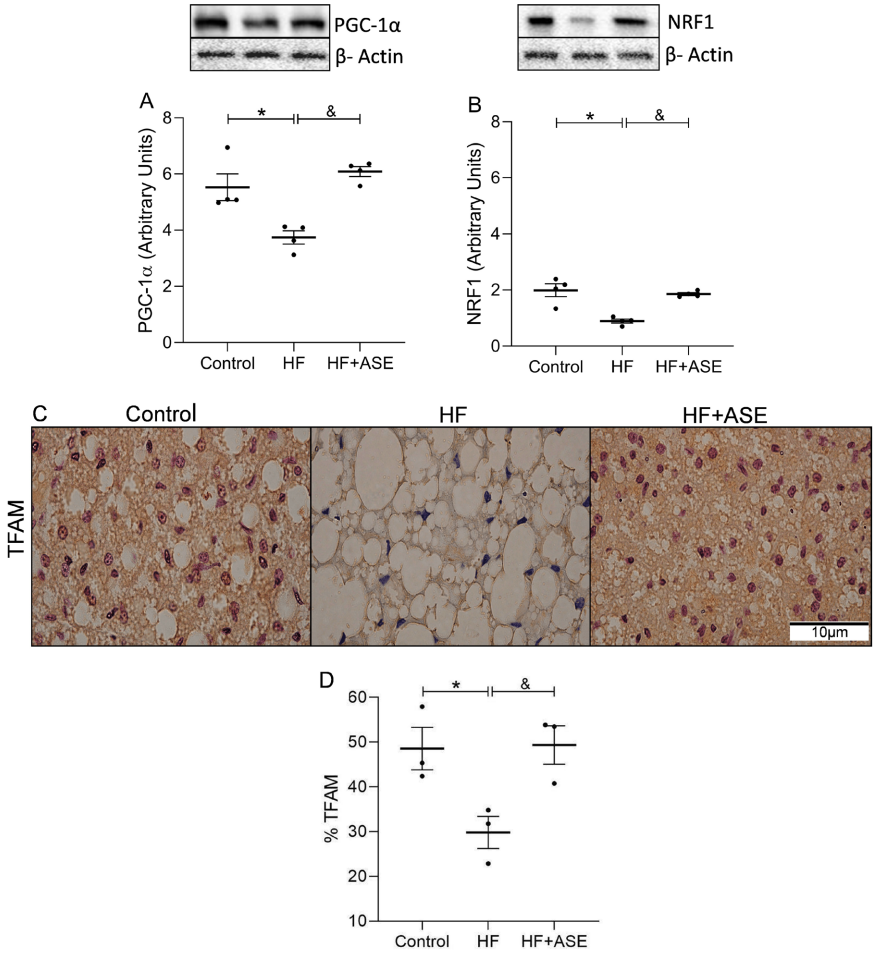

Figure 4. Mitochondrial biogenesis markers. Effects of ASE on the expression of PGC-1*α*, n = 4 (A), NRF1, n = 4 (B), TFAM immunostaining (C), and % of TFAM, n = 3 (D) in brown adipose tissue from HFD-fed mice. The photomicrograph is shown at 100x, with a scale bar of 10 μm. Values are presented as means ± SEM. One-way ANOVA analyses, and post-test of Tukey indicate *significantly different from the control group ($p \leq 0.05$), and &significantly different from the corresponding HF group ($p \leq 0.05$).

3.7. Effect of ASE on Oxidant Status

The indicators of lipid peroxidation, 8-isoprostane and MDA, were evaluated to determine oxidative damage, and the antioxidant enzymes SOD, CAT, and GPx were assessed to observe protection against the formation of ROS. Although there was no significant increase in 8-isoprostane staining in BAT slides from the HF compared to the Control group (**Figure 5(A)** and **Figure 5(B)**), treatment with ASE reduced the immunostaining ($p = 0.0338$) compared to the HF group. BAT homogenate of the HF group showed a substantial increase in MDA levels (**Figure 5(C)**) compared to the Control group ($p = 0.0092$). The ASE treatment demonstrated a significant protective effect ($p = 0.0017$) against these elevated MDA levels in the treated animals compared to the HF group.

Antioxidant status was determined by SOD, CAT, and GPx activity in BAT homogenate. The HF group demonstrated a significant reduction in the activity of

the antioxidant enzymes SOD ($p = 0.0158$) (Figure 5(D)) and CAT ($p = 0.0291$) (Figure 5(E)) compared to the Control group. The treatment with ASE prevented only the reduction of SOD activity ($p = 0.0180$), not significantly altering CAT activity. Regarding GPx activity (Figure 5(F)), no significant difference was observed between the analyzed groups.

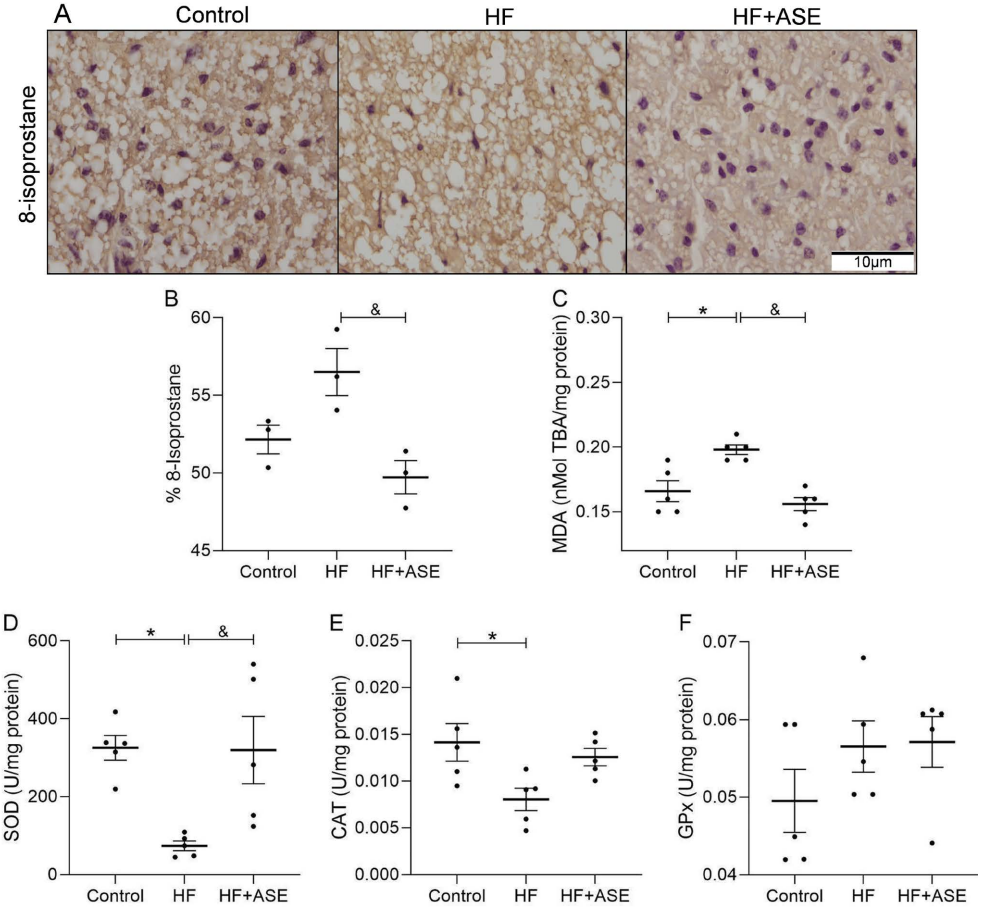

Figure 5. Oxidative status. Effects of ASE on 8-isoprostane immunostaining (A), % of 8-isoprostane, n = 3 (B), MDA levels, n = 5 (C), and antioxidant activity of SOD, n = 5 (D), CAT, n = 5 (E) and GPx, n = 5 (F) in brown adipose tissue from HF-fed mice. The photomicrograph is shown at 100x, with a scale bar of 10 µm. Values are presented as means ± SEM. One-way ANOVA analyses, and post-test of Tukey indicate *significantly different from the control group ($p \leq 0.05$), and &significantly different from the corresponding HF group ($p \leq 0.05$).

3.8. Effect of ASE on Inflammation Markers

Pro-inflammatory cytokines IL-6, MCP-1, and TNF-α were stained in BAT slides to evaluate the effects of ASE on inflammation. The HF group showed a significant increase in the staining of the pro-inflammatory cytokines IL-6 ($p = 0.0251$) (Figure 6(A) and Figure 6(B)), MCP-1 ($p = 0.0237$) (Figure 6(A) and Figure 6(C)), and TNF-α ($p = 0.0103$) (Figure 6(A) and Figure 6(D)) compared to the Control group. Treatment with ASE reduced the MCP-1 ($p = 0.0038$) and TNF-α ($p = 0.0244$) staining, but not IL-6, compared to the HF group.

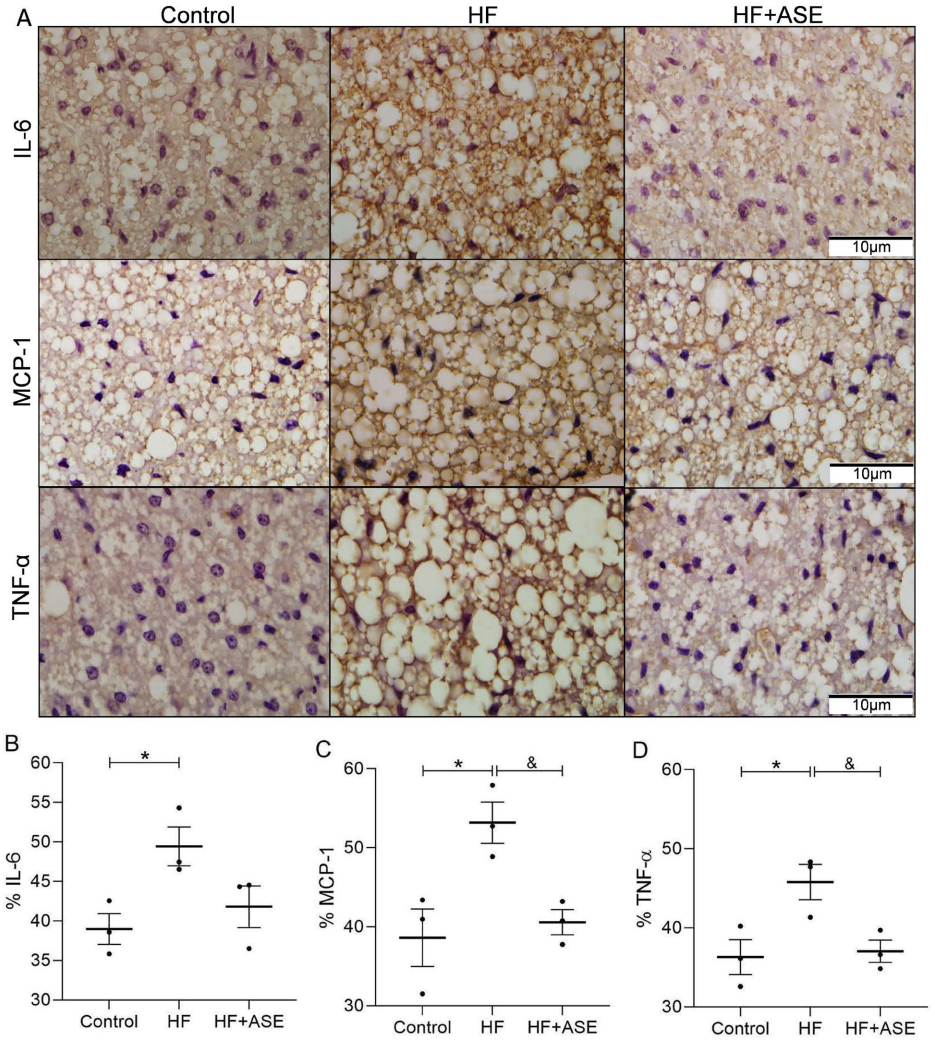

Figure 6. Oxidative status. Effects of ASE on 8-isoprostane immunostaining (A), % of 8-isoprostane, n = 3 (B), MDA levels, n = 5 (C), and antioxidant activity of SOD, n = 5 (D), CAT, n = 5 (E) and GPx, n = 5 (F) in brown adipose tissue from HF-fed mice. The photomicrograph is shown at 100x, with a scale bar of 10 μm. Values are presented as means ± SEM. One-way ANOVA analyses, and post-test of Tukey indicate *significantly different from the control group ($p \leq 0.05$), and &significantly different from the corresponding HF group ($p \leq 0.05$).

4. Discussion

The present study demonstrates that chronic consumption of an HF diet induces classical features of diet-induced obesity in C57BL/6 mice, including increased body weight, adiposity, hyperglycemia, and dyslipidemia [16]-[18]. Treatment with ASE was able to prevent these alterations without affecting energy intake, which is reinforced by the improvement in metabolic efficiency. These significant findings, which corroborate previous data from our group, indicate that the polyphenol-rich extract from *Euterpe oleracea* exerts anti-obesogenic effects by modulating adipose tissue metabolism and improving systemic metabolic parameters [16]-[18].

The growing body of evidence supports BAT as a potential new target for treating obesity-induced disorders [30]. In line with the preventive scope of this study, a central finding is the preservation of BAT structure and function by ASE. BAT is known to play a crucial role in energy expenditure through thermogenesis. Obesity leads to BAT dysfunction, often characterized by whitening, increased lipid accumulation, and reduced mitochondrial density [5] [6].

The present results showed that HFD induces BAT hypertrophy, increasing tissue mass and adipocyte size by enhancing lipid infiltration and reducing the nuclear density in this tissue, which aligns with previous findings [31] [32]. However, it is the first evidence showing ASE's effect on BAT morphology, preventing the above alterations and preserving the multilocular structure in the BAT of HF-fed mice. Previous studies have demonstrated the activity of other compounds on BAT remodeling, such as eicosapentaenoic acid (EPA), docosahexaenoic acid (DHA), and fenofibrate [6] [31] [33]. Therefore, these findings suggest that ASE is beneficial in preventing BAT dysfunction and also highlight its potential for therapeutic application.

BAT activation enhances lipid metabolism and promotes the release of free fatty acids (FFA), a crucial fuel for thermogenesis and a direct activator of UCP-1 [34]. Mechanistically, the protective effects of ASE appear to be linked to improved lipid mobilization and mitochondrial function in BAT. ASE increased the expression of key lipolytic proteins (ATGL, HSL, PLIN-1) and thermogenic markers (UCP-1, β_3-AR), which are typically suppressed in obesity. Thus, these results suggest a possible reactivation of thermogenesis pathways. ASE treatment also restored the expression of PPARα, a well-known transcriptional factor that regulates lipid metabolism and induces UCP-1 expression, mitochondrial biogenesis, and β-oxidation [6]. Although we did not directly assess thermogenic activity, our results are consistent with the hypothesis that ASE supports BAT function through a PPARα-dependent mechanism.

Additionally, ASE prevented the downregulation of mitochondrial biogenesis markers (PGC-1α, NRF1, and TFAM) in BAT promoted by obesity, which is consistently associated in the literature with impaired mitochondrial biogenesis and function, a phenomenon also observed in our HF-fed animals [6] [35]. Notably, PGC1-α plays a central role in maintaining mitochondrial function, as it coordinates the expression of mitochondrial DNA by promoting TFAM expression, with the support of NRF1 [36]. These findings indicate that ASE not only preserves BAT morphology but also sustains its mitochondrial integrity, a hallmark of its thermogenic capacity. Polyphenol-rich extracts are known to activate the PGC-1α/NRF1/TFAM pathway, lead to the synthesis of new mitochondria [8] [36], and improve mitochondrial function, which may partly explain the effects observed in this study [7].

Mitochondrial dysfunction in BAT is often accompanied by oxidative stress and low-grade inflammation, both of which are exacerbated by obesity. The HFD increased lipid peroxidation (MDA) and reduced antioxidant enzyme activities (SOD, CAT), while also promoting inflammation via increased expression of IL-

6, MCP-1, and TNF-α and related brown adipocyte dysfunction [9] [35]-[37]. The whitening process observed in BAT may explain the secretion of pro-inflammatory cytokines. Moreover, previous data indicate that low-grade inflammation in BAT contributes to excessive ROS production and is associated with oxidative stress in this tissue [9].

In this study, in addition to its metabolic regulation, ASE also exhibited antioxidant and anti-inflammatory effects in BAT, thereby attenuating oxidative damage and restoring SOD activity while reducing MCP-1 and TNF-α levels. These results are consistent with the known anti-inflammatory and antioxidant actions of Euterpe oleracea polyphenols in other tissues [16]-[18] [21] [38] [39].

Despite the promising results observed, some limitations should be acknowledged to contextualize the findings better and guide future research. A key limitation of the study is the lack of direct assessment of BAT thermogenic activity. Future studies should include functional assays to confirm whether the increased expression of thermogenic proteins translates into enhanced energy expenditure. Furthermore, only male mice were studied. However, given the relevance of studying metabolic changes induced by HFD, the effects of ASE in females remain to be explored.

5. Conclusions

In conclusion, ASE effectively prevented weight gain, visceral adiposity, blood glucose elevation, and intra-abdominal adipose tissue mass increase in C57Bl/6 mice fed an HFD. Together, our data demonstrate that ASE supports metabolic health through a combination of complementary actions, including limiting fat accumulation, preserving the structure and function of BAT, enhancing mitochondrial biogenesis, and stimulating lipolysis and thermogenic signaling. The anti-inflammatory and antioxidant action of ASE observed in BAT suggests an additional beneficial mechanism in the dysfunction of this tissue and the metabolic changes associated with obesity. These results support ASE as a promising natural source for treating obesity using BAT as a new target.

Funding Sources

This work was supported by the National Council of Scientific and Technological Development/CNPq (grant number 304381/2021-7), and the Rio de Janeiro State Research Agency/FAPERJ (grant numbers E-26/200.931/2021, E-26/211.287/2021).

Acknowledgements

The authors are grateful to the technical support staff of the Laboratory of Cardiovascular Pharmacology and Medicinal Plants at the Rio de Janeiro State University (UERJ) for their valuable assistance throughout the study. D.L.B.S acknowledges the Coordination for the Improvement of Higher Education Personnel (CAPES) and the Rio de Janeiro State Research Foundation (FAPERJ) for the master's scholarship.

Conflicts of Interest

The authors declare no conflicts of interest regarding the publication of this paper.

References

[1] Blüher, M. (2025) An Overview of Obesity-Related Complications: The Epidemiological Evidence Linking Body Weight and Other Markers of Obesity to Adverse Health Outcomes. *Diabetes, Obesity and Metabolism*, **27**, 3-19. https://doi.org/10.1111/dom.16263

[2] Bhatt, P.S., Dhillo, W.S. and Salem, V. (2017) Human Brown Adipose Tissue—Function and Therapeutic Potential in Metabolic Disease. *Current Opinion in Pharmacology*, **37**, 1-9. https://doi.org/10.1016/j.coph.2017.07.004

[3] Boon, M.R. and van Marken Lichtenbelt, W.D. (2015) Brown Adipose Tissue: A Human Perspective. In: Herzig, S., Ed., *Metabolic Control*, *Handbook of Experimental Pharmacology*, Springer International Publishing, 301-319. https://doi.org/10.1007/164_2015_11

[4] Chait, A. and den Hartigh, L.J. (2020) Adipose Tissue Distribution, Inflammation and Its Metabolic Consequences, Including Diabetes and Cardiovascular Disease. *Frontiers in Cardiovascular Medicine*, **7**, Article No. 22. https://doi.org/10.3389/fcvm.2020.00022

[5] Bartelt, A. and Heeren, J. (2013) Adipose Tissue Browning and Metabolic Health. *Nature Reviews Endocrinology*, **10**, 24-36. https://doi.org/10.1038/nrendo.2013.204

[6] Miranda, C.S., Silva-Veiga, F., Martins, F.F., Rachid, T.L., Mandarim-De-Lacerda, C.A. and Souza-Mello, V. (2020) PPAR-α Activation Counters Brown Adipose Tissue Whitening: A Comparative Study between High-Fat- and High-Fructose-Fed Mice. *Nutrition*, **78**, Article ID: 110791. https://doi.org/10.1016/j.nut.2020.110791

[7] Diaz-Vegas, A., Sanchez-Aguilera, P., Krycer, J.R., Morales, P.E., Monsalves-Alvarez, M., Cifuentes, M., *et al.* (2020) Is Mitochondrial Dysfunction a Common Root of Noncommunicable Chronic Diseases? *Endocrine Reviews*, **41**, bnaa005. https://doi.org/10.1210/endrev/bnaa005

[8] Wood dos Santos, T., Cristina Pereira, Q., Teixeira, L., Gambero, A., A. Villena, J. and Lima Ribeiro, M. (2018) Effects of Polyphenols on Thermogenesis and Mitochondrial Biogenesis. *International Journal of Molecular Sciences*, **19**, Article No. 2757. https://doi.org/10.3390/ijms19092757

[9] Omran, F. and Christian, M. (2020) Inflammatory Signaling and Brown Fat Activity. *Frontiers in Endocrinology*, **11**, Article No. 156. https://doi.org/10.3389/fendo.2020.00156

[10] Armani, A., Feraco, A., Camajani, E., Gorini, S., Lombardo, M. and Caprio, M. (2022) Nutraceuticals in Brown Adipose Tissue Activation. *Cells*, **11**, Article No. 3996. https://doi.org/10.3390/cells11243996

[11] Negi, H., Gupta, M., Walia, R., Khataibeh, M. and Sarwat, M. (2021) Medicinal Plants and Natural Products: More Effective and Safer Pharmacological Treatment for the Management of Obesity. *Current Drug Metabolism*, **22**, 918-930. https://doi.org/10.2174/1389200222666210729114456

[12] Vannuchi, N. and Pisani, L. (2025) PGC-1α Activation by Polyphenols: A Pathway to Thermogenesis. *Molecular Nutrition & Food Research*, **69**, e70072. https://doi.org/10.1002/mnfr.70072

[13] Hachemi, I. and U-Din, M. (2023) Brown Adipose Tissue: Activation and Metabo-

lism in Humans. *Endocrinology and Metabolism*, **38**, 214-222. https://doi.org/10.3803/enm.2023.1659

[14] de Moura, R.S. and Resende, Â.C. (2016) Cardiovascular and Metabolic Effects of Açaí, an Amazon Plant. *Journal of Cardiovascular Pharmacology*, **68**, 19-26. https://doi.org/10.1097/fjc.0000000000000347

[15] Rocha, A.P.M., Carvalho, L.C.R.M., Sousa, M.A.V., Madeira, S.V.F., Sousa, P.J.C., Tano, T., *et al.* (2007) Endothelium-Dependent Vasodilator Effect of *Euterpe oleracea* Mart. (Açaí) Extracts in Mesenteric Vascular Bed of the Rat. *Vascular Pharmacology*, **46**, 97-104. https://doi.org/10.1016/j.vph.2006.08.411

[16] de Oliveira, P.R.B., da Costa, C.A., de Bem, G.F., Cordeiro, V.S.C., Santos, I.B., de Carvalho, L.C.R.M., *et al.* (2015) *Euterpe oleracea* Mart.-Derived Polyphenols Protect Mice from Diet-Induced Obesity and Fatty Liver by Regulating Hepatic Lipogenesis and Cholesterol Excretion. *PLOS ONE*, **10**, e0143721. https://doi.org/10.1371/journal.pone.0143721

[17] Romão, M.H., de Bem, G.F., Santos, I.B., de Andrade Soares, R., Ognibene, D.T., de Moura, R.S., *et al.* (2020) Açaí (*Euterpe oleracea* Mart.) Seed Extract Protects against Hepatic Steatosis and Fibrosis in High-Fat Diet-Fed Mice: Role of Local Renin-Angiotensin System, Oxidative Stress and Inflammation. *Journal of Functional Foods*, **65**, Article ID: 103726. https://doi.org/10.1016/j.jff.2019.103726

[18] Santos, I.B., de Bem, G.F., da Costa, C.A., de Carvalho, L.C.R.M., de Medeiros, A.F., Silva, D.L.B., *et al.* (2020) Açaí Seed Extract Prevents the Renin-Angiotensin System Activation, Oxidative Stress and Inflammation in White Adipose Tissue of High-Fat Diet-Fed Mice. *Nutrition Research*, **79**, 35-49. https://doi.org/10.1016/j.nutres.2020.05.006

[19] Singleton, V.L. and Rossi, J.A. (1965) Colorimetry of Total Phenolics with Phosphomolybdic-Phosphotungstic Acid Reagents. *American Journal of Enology and Viticulture*, **16**, 144-158. https://doi.org/10.5344/ajev.1965.16.3.144

[20] de Moura, R.S., Pires, K.M.P., Ferreira, T.S., Lopes, A.A., Nesi, R.T., Resende, A.C., *et al.* (2011) Addition of Açaí (*Euterpe oleracea*) to Cigarettes Has a Protective Effect against Emphysema in Mice. *Food and Chemical Toxicology*, **49**, 855-863. https://doi.org/10.1016/j.fct.2010.12.007

[21] de Moraes Arnoso, B.J., Magliaccio, F.M., de Araújo, C.A., de Andrade Soares, R., Santos, I.B., de Bem, G.F., *et al.* (2022) Açaí Seed Extract (ASE) Rich in Proanthocyanidins Improves Cardiovascular Remodeling by Increasing Antioxidant Response in Obese High-Fat Diet-Fed Mice. *Chemico-Biological Interactions*, **351**, Article ID: 109721. https://doi.org/10.1016/j.cbi.2021.109721

[22] Martins, F., Campos, D.H.S., Pagan, L.U., Martinez, P.F., Okoshi, K., Okoshi, M.P., *et al.* (2015) High-Fat Diet Promotes Cardiac Remodeling in an Experimental Model of Obesity. *Arquivos Brasileiros de Cardiologia*, **105**, 479-486. https://doi.org/10.5935/abc.20150095

[23] Taylor, B.A. and Phillips, S.J. (1996) Detection of Obesity QTLs on Mouse Chromosomes 1 and 7 by Selective DNA Pooling. *Genomics*, **34**, 389-398. https://doi.org/10.1006/geno.1996.0302

[24] de Bem, G.F., da Costa, C.A., da Silva Cristino Cordeiro, V., Santos, I.B., de Carvalho, L.C.R.M., de Andrade Soares, R., *et al.* (2018) *Euterpe oleracea* Mart. (açaí) Seed Extract Associated with Exercise Training Reduces Hepatic Steatosis in Type 2 Diabetic Male Rats. *The Journal of Nutritional Biochemistry*, **52**, 70-81. https://doi.org/10.1016/j.jnutbio.2017.09.021

[25] Xavier, H.T., Izar, M.C., Faria Neto, J.R., Assad, M.H., Rocha, V.Z., Sposito, A.C., *et*

al. (2013) V Diretriz Brasileira de Dislipidemias e Prevenção da Aterosclerose. *Arquivos Brasileiros de Cardiologia*, **101**, 1-22. https://doi.org/10.5935/abc.2013s010

[26] Draper, H.H. and Hadley, M. (1990) Malondialdehyde Determination as Index of Lipid Peroxidation. In: *Methods in Enzymology*, Elsevier, 421-431. https://doi.org/10.1016/0076-6879(90)86135-i

[27] Bannister, J.V. and Calabrese, L. (1987) Assays for Superoxide Dismutase. In: Glick, D., Ed., *Methods of Biochemical Analysis*, Wiley, 279-312. https://doi.org/10.1002/9780470110539.ch5

[28] Aebi, H. (1984) Catalase *in Vitro*. In: *Methods in Enzymology*, Elsevier, 121-126. https://doi.org/10.1016/s0076-6879(84)05016-3

[29] Flohé, L. and Günzler, W.A. (1984) Assays of Glutathione Peroxidase. In: *Methods in Enzymology*, Elsevier, 114-120. https://doi.org/10.1016/s0076-6879(84)05015-1

[30] Fernández-Verdejo, R., Marlatt, K.L., Ravussin, E. and Galgani, J.E. (2019) Contribution of Brown Adipose Tissue to Human Energy Metabolism. *Molecular Aspects of Medicine*, **68**, 82-89. https://doi.org/10.1016/j.mam.2019.07.003

[31] Bargut, T.C.L., Martins, F.F., Santos, L.P., Aguila, M.B. and Mandarim-de-Lacerda, C.A. (2019) Administration of Eicosapentaenoic and Docosahexaenoic Acids May Improve the Remodeling and Browning in Subcutaneous White Adipose Tissue and Thermogenic Markers in Brown Adipose Tissue in Mice. *Molecular and Cellular Endocrinology*, **482**, 18-27. https://doi.org/10.1016/j.mce.2018.12.003

[32] Rangel-Azevedo, C., Santana-Oliveira, D.A., Miranda, C.S., Martins, F.F., Mandarimde-Lacerda, C.A. and Souza-Mello, V. (2022) Progressive Brown Adipocyte Dysfunction: Whitening and Impaired Nonshivering Thermogenesis as Long-Term Obesity Complications. *The Journal of Nutritional Biochemistry*, **105**, Article ID: 109002. https://doi.org/10.1016/j.jnutbio.2022.109002

[33] Rachid, T.L., Penna-de-Carvalho, A., Bringhenti, I., Aguila, M.B., Mandarim-de-Lacerda, C.A. and Souza-Mello, V. (2015) Fenofibrate (PPARalpha Agonist) Induces Beige Cell Formation in Subcutaneous White Adipose Tissue from Diet-Induced Male Obese Mice. *Molecular and Cellular Endocrinology*, **402**, 86-94. https://doi.org/10.1016/j.mce.2014.12.027

[34] Gharanei, S., Shabir, K., Brown, J.E., Weickert, M.O., Barber, T.M., Kyrou, I., *et al.* (2020) Regulatory microRNAs in Brown, Brite and White Adipose Tissue. *Cells*, **9**, Article No. 2489. https://doi.org/10.3390/cells9112489

[35] Shabalina, I.G., Vrbacký, M., Pecinová, A., Kalinovich, A.V., Drahota, Z., Houštěk, J., *et al.* (2014) ROS Production in Brown Adipose Tissue Mitochondria: The Question of UCP1-Dependence. *Biochimica et Biophysica Acta* (*BBA*)-*Bioenergetics*, **1837**, 2017-2030. https://doi.org/10.1016/j.bbabio.2014.04.005

[36] Chodari, L., Dilsiz Aytemir, M., Vahedi, P., Alipour, M., Vahed, S.Z., Khatibi, S.M.H., *et al.* (2021) Targeting Mitochondrial Biogenesis with Polyphenol Compounds. *Oxidative Medicine and Cellular Longevity*, **2021**, Article ID: 4946711. https://doi.org/10.1155/2021/4946711

[37] Roberts-Toler, C., O'Neill, B.T. and Cypess, A.M. (2015) Diet-Induced Obesity Causes Insulin Resistance in Mouse Brown Adipose Tissue. *Obesity*, **23**, 1765-1770. https://doi.org/10.1002/oby.21134

[38] de Moura, R.S., Ferreira, T.S., Lopes, A.A., Pires, K.M.P., Nesi, R.T., Resende, A.C., *et al.* (2012) Effects of *Euterpe oleracea* Mart. (AÇAÍ) Extract in Acute Lung Inflammation Induced by Cigarette Smoke in the Mouse. *Phytomedicine*, **19**, 262-269. https://doi.org/10.1016/j.phymed.2011.11.004

[39] de Oliveira, P.R.B., da Costa, C.A., de Bem, G.F., Marins de Cavalho, L.C.R., de Souza, M.A.V., de Lemos Neto, M., *et al.* (2010) Effects of an Extract Obtained from Fruits of *Euterpe oleracea* Mart. in the Components of Metabolic Syndrome Induced in C57BL/6J Mice Fed a High-Fat Diet. *Journal of Cardiovascular Pharmacology*, **56**, 619-626. https://doi.org/10.1097/fjc.0b013e3181f78da4

Supplementary Material

Table S1. Diets composition.

Nutrients (U/Kg diet)	Standard Diet	High-fat Diet
Casein (g)	148	190
Corn strach (g)	620.7	250.7
Sucrose (g)	100	100
Soybean oil (g)	40	40
Lard (g)	-	320
Fibers (g)	50	50
Mineral mix (g)	35	35
Vitamin mix (g)	10	10
L-cystine (g)	1.8	1.8
Choline chloride (g)	2.5	2.5
Energy (kcal)	3.800	5.400
***Carbohydrate* (%)**	**76**	**26**
***Protein* (%)**	**14**	**14**
***Lipids* (%)**	**10**	**60**

Composition of the standard and high-fat diets offered to the animals during the experimental protocol. Both diets were balanced and produced by Rhoster Indústria e Comércio Ltda. (Araçoiaba da Serra, SP, Brazil). The vitamin and mineral mix followed the AIN-93M recommendations for adult rodents.

Table S2. Primary antibodies used for immunohistochemistry.

Target Protein	Host species	Dilution	Supplier (Catalog No.)	Location
8-Isoprostane	Goat	1:100	Oxford Biomedical (-)	Oxford, UK
IL-6	Goat	1:100	Santa Cruz Biotech (sc-1265)	Dallas, TX, USA
MCP-1	Goat	1:100	Santa Cruz Biotech (sc-1785)	Dallas, TX, USA
TNF-α	Mouse	1:100	Santa Cruz Biotech (sc-52746)	Dallas, TX, USA
TFAM	Rabbit	1:100	Boster Bio (PB9447)	Pleasanton, CA, USA
UCP-1	Rabbit	1:100	Cusabio (CSB-PA05554ESR2HU)	Houston, TX, USA

Primary antibodies used for immunohistochemistry in brown adipose tissue (BAT) included: goat anti-8-isoprostane (8-epi-PGF2α), goat anti-interleukin-6 (IL-6), goat anti-monocyte chemoattractant protein-1 (MCP-1), mouse anti-tumor necrosis factor-alpha (TNF-α), rabbit anti-mitochondrial transcription factor A (TFAM), and rabbit anti-uncoupling protein 1 (UCP-1). All antibodies were incubated overnight at 4 ˚C in a humidified chamber, as detailed in the Methods section.

Table S3. Primary antibodies used for western blot.

Target Protein	Host species	Dilution	Supplier (Catalog No.)	Location
β_3-AR	Rabbit	1:500	Bioss Inc. (BS-10921R)	Woburn, MA, USA
PPARα	Rabbit	1:500	Santa Cruz Biotech (sc-9000)	Houston, TX, USA
PLIN-1	Rabbit	1:1000	Cusabio (CSB-PA937313)	Houston, TX, USA
ATGL	Rabbit	1:1000	Cusabio (CSB-PA836180LAO1HU)	Houston, TX, USA
HSL	Rabbit	1:1000	Cusabio (CSB-PA009841)	Pleasanton, CA, USA
PGC1-α	Rabbit	1:500	Santa Cruz Biotech (sc-13067)	Dallas, TX, USA
NRF1	Rabbit	1:1000	Cusabio (CSB-PA009841)	Houston, TX, USA
β-actin	Mouse	1:1000	Santa Cruz Biotech (sc-47778)	Dallas, TX, USA

Primary antibodies used for Western blot analysis included: rabbit anti-β_3-adrenergic receptor (β_3-AR), rabbit anti-peroxisome proliferator-activated receptor alpha (PPARα), rabbit anti-perilipin 1 (PLIN-1), rabbit anti-adipose triglyceride lipase (ATGL), rabbit anti-hormone-sensitive lipase (HSL), rabbit anti-peroxisome proliferator-activated receptor gamma coactivator 1-alpha (PGC1-α), rabbit anti-nuclear respiratory factor 1 (NRF1), and mouse anti-β-actin (used as a loading control). All primary antibodies were incubated overnight at 4 ˚C under constant agitation, as detailed in the Methods section.

HPLC Analysis and MALDI-TOF Mass Spectrum of ASE

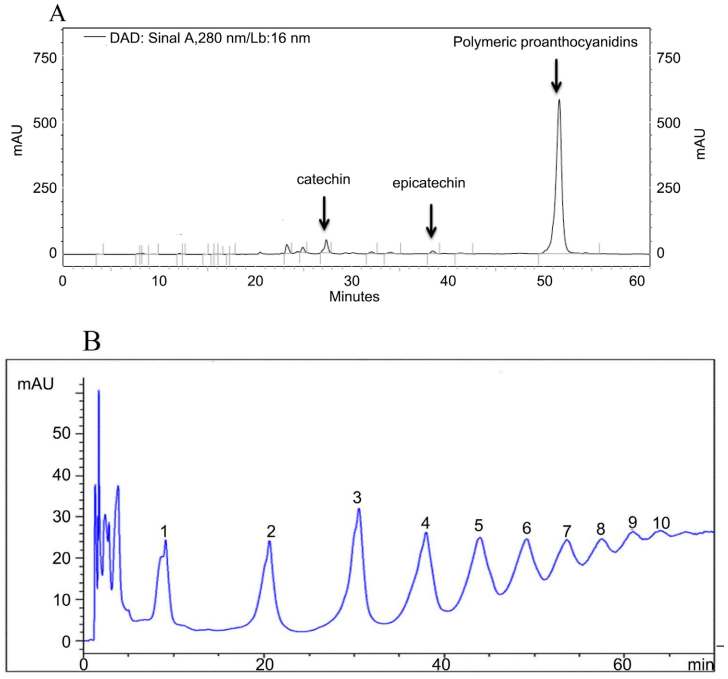

Figure S1. HPLC analysis of ASE. (A) HPLC analysis of the aqueous residue of ASE according to Peng, *et al.* (2001) [1]. The marked peaks of 27, 38 and 51 min correspond to catechin, epicatechin and oligomeric and polymeric condensed tannins. (B) HPLC analysis of the aqueous fraction residue according to Kelm, *et al.* (2006) [2], where the marked peaks (1 to 10) show the series of condensed tannins present in the sample from monomer to decamer.

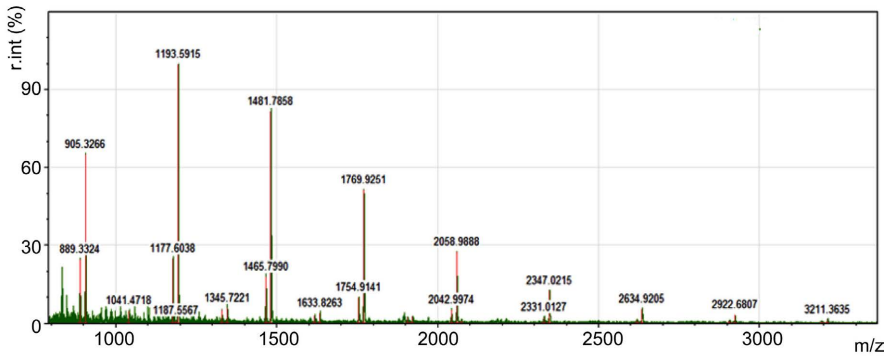

Figure S2. MALDI-TOF mass spectrum of the aqueous fraction residue from ASE.

The spectrum was obtained on a Bruker Autoflex Speed; DHB matrix, 1:1:10 (sample: NaCl: matrix). Mass peaks are of sodium adducts of B-type proanthocyanidins: [M + Na] + m/z = 889, 903, 1177, 1193, 1465, 1481, 1753, 1769, 2041, 2058, 2329, 2347, 2617, 2634, 2907, 2922, 3193 and 3211.